Global Research journal of Natural Science and Technology (Grjnst)
Volume: 03 - Issue 3 (2025)
p.ISSN: 2790-7643 e.ISSN: 2790-7651
www.grjnst.com

Discrete Element Simulations of Drag Force Acting on Spherical Intruder Moving in Static Granular Media

Ram Chand *

Department of Natural Sciences, The Begum Nusrat Bhutto Women University, Sukkur, Sindh, Pakistan

ram.chand@bnbwu.edu.pk

Shahzad Nasim

The Begum Nusrat Bhutto Women University, Sukkur, Sindh, Pakistan

shahzad.nasim@bnbwu.edu.pk

Saeed Uddin

Hyderabad Institute for Technology & Management Sciences, Hyderabad, Sindh, Pakistan

rectorhitmshyd@gmail.com

Iqra

The Begum Nusrat Bhutto Women University, Sukkur, Sindh, Pakistan

Iqra3.20mh004@bnbwu.edu.pk

Sajjad Hussain

The Begum Nusrat Bhutto Women University, Sukkur, Sindh, Pakistan

sajjad.hussain@bnbwu.edu.pk

*ram.chand@bnbwu.edu.pk**

**corresponding author*

Abstract

This paper presents a discrete element method (DEM) simulation of the drag force experienced by spherical shaped intruder moving along different paths in confined granular media. It is revealed that the drag force depends upon friction of both wall-particle and particle-particle and force profile is also affected by nearby walls. We also confirmed that the arch formation in the granular media is responsible for this peculiar behavior.

Keywords: Static Granular; Discrete Element Method; Force Profile; Janssen Model.

Introduction

The granular media have long been a research field of the engineering and scientific communities; however, their static and dynamic properties are still not fully understood [1–3]. Granular materials are the second most frequently used media after water; therefore, any improved knowledge in this field potentially leads to numerous economic benefits. In addition to industrial applications, such materials interest physicists since they exhibit certain properties which are not fully understood. To investigate these properties of granular media, such as propagation of force and stress distribution, many experimental and numerical techniques have emerged. One of them is to investigate the force experienced by intruders in granular media. Objects moving vertically in static granular media experience drag and plunging forces [4,5]. These forces depend upon how and where the object is moving in granular media.

Many researchers have been studying the force profile of an intruder in a static granular bed both experimentally and numerically [6]. It was found experimentally found that the drag force on the intruder was dependent on both the geometry and the depth of the intruder. Drag force on a plate moving vertically in a granular bed and found has been studied by [7,8]. They

found that the initial linear profile is due to hydrostatics, while the depth-dependent profile is similar to the one predicted by Janssen Model [9]. Other researchers have also found that plunging and withdrawing forces depend on the depth, intruder's geometry and also the location in the granular medium rather than on intruder's velocity [15] experimentally measured the force on different size and shape of intruder motion vertically in the disordered media. Their results showed that the force profiles of fully immersed intruders have the concave-to-convex transition and that sidewalls of the container are not responsible for force-profile of an intruder. While studies on drag induced lift force, drag force and plunging force have been carried out [16–18], however there has been a little work on forces on object motion near walls. Moreover, the force on spherical intruder motion vertically up in granular bed has not been explored fully.

The paper focuses on the numerical determination of the drag force acting on horizontally and vertically moving spherical-shaped intruders in static granular media by utilizing 3D DEM. Two types of testing have been carried out, in the first case, an intruder was allowed to move in cylindrical granular packing and the second case intruder was moved in rectangular granular packing in all types of simulation and these simulations are unlike other simulators [17,19]. The simulation result shows that the drag force depends upon friction between wall-particle and particle-particle, also it is revealed that force-profile varies with moving near walls. In addition, the intruder experiences strong drag forces near walls as compared to motions in depth of the bed. Finally, this study also verifies that stresses on vertical wall increase as height increases in accordance with Janssen Model [9].

Fig 1 shows the shape of the "facing" track of the drag body and the shape of the "countercurrent" direction simultaneously affect the drag force. Specifically, the sharper the

"facing" surface, the lesser the drag resistance, the flatter the "countercurrent" surface, smaller the drag resistance. essentially, the weight of the impact of the shape of the "catch-up" The drag body's direction is significantly larger than the impact of the shape of the "countercurrent" direction.

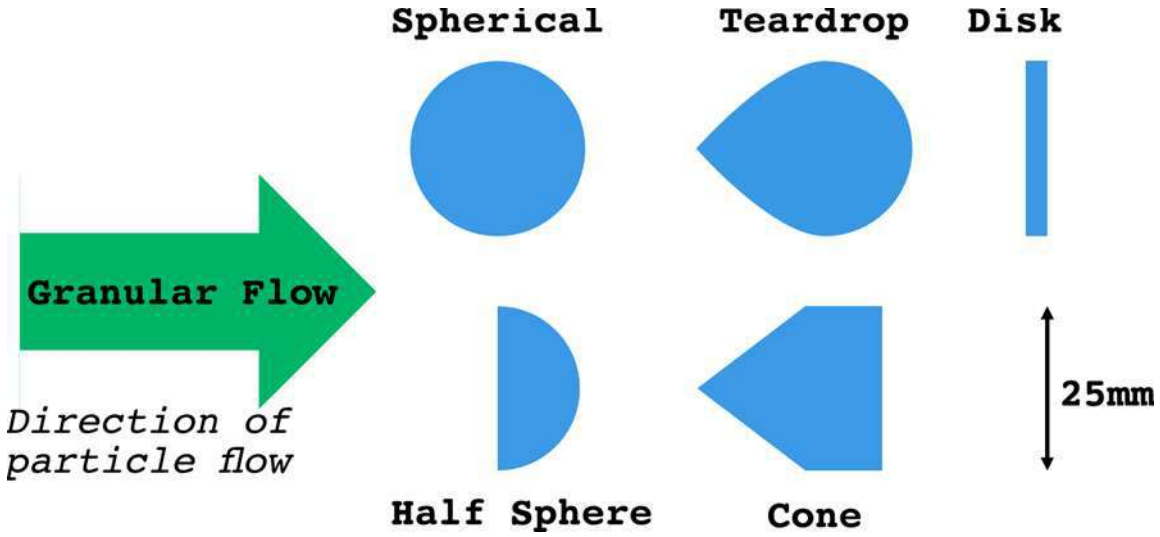

Fig. 1 Different intruder shapes and the direction of granular flow, highlighting the greater impact of the facing surface shape on drag reduction..

Soller et. al. [5] used a cube to rotate around the central axis in a particle bed and analyzed the association among the rotational moment and the thickness, width, depth of invasion, and particle diameter of the cube. Studies have shown that this rotational moment is proportional to the generalized intrusion depth (the sum of the actual intrusion depth of the drag body and the particle diameter) and the general diagonal of the rectangular transverse section (refers to the actual geometric diagonal dimension of the drag body and the cube of the particle diameter is proportional to the cube. Cavarretta et. al. [22] used a self-developed instrument to precisely assess the rigidity and friction coefficient of sand grains and established a corresponding model. Through its research, it is found that the particle shape

and surface roughness have a great influence on the mechanical properties of the granular material.

Umbanhowar et. al. [19] proposed the concept of a typical compaction rate. At this typical compaction rate, the particles are neither dilatant nor sheared. Above this value, the drag force increases as the density increases, and below this value, the drag force does not substantially change. The accumulation of particles in front of the drag body is a wave geometry. Researchers have also discovered that the connection between the velocity and the drag force conformed to the quadratic function law [9], while in [7] it was revealed that the drag force increased linearly with speed and in [24] it was observed that the drag force did not change with speed. However, how the low force direction affects the influence of the force direction on the drag requires further study. In addition, further study is also necessary to investigate the relations of the spherical drag body, such as its diameter is proportional to the depth of invasion.

1.1. Discrete Element Method (DEM)

DEM are numerical tools for simulating soil and other granules. It is special in that it accurately considers the individual particles as well as the interaction between the particles. DEM provides a new way of thinking about the study of particulate materials. DEM simulations range from food technology to mining engineering [10,11]. Zhu et al. [28] classified DEM into two categories: one is a soft sphere model and the other is a hard-sphere model. The so-called softball model is to allow the particles to contact each other “piercing”, whereas the so-called hardball model is not allowed to deform the particles. What these two

models have in common is that they are time-dependent, which means that changes within the granular system can be extrapolated over time in a time period.

This method, which is coded initially by Cundall and Strack [12], is very similar to the process of other numerical simulations. The difference is that the post-processing of discrete elements varies from software to software. Unlike the continuum mechanics method, the discrete element does not require the constitutive model of the material as an input parameter, but the contact model between the particles is indispensable because it relates the macroscopic response of the particle to the external force. Therefore, the constitutive model of the granules can be summarized by the simulation results of the discrete elements. It is important to note that the particle-level contact model and the macroscopic constitute model of the granule are not suitable or difficult to establish a one-to-one correspondence. For example, even with a linear elastic particle contact model, the macroscopic effects are likely to be nonlinear.

In this model, the particle motion as well as the different interactions are calculated by Newtonian equations of motion. The net force on each spherical particle (i) is determined by the sum of gravitational and inter-particle components:

$$\sum F_i = m_i g + F_n + F \ldots\ldots\ldots\ldots (1)$$

where F_n and F_t are normal and tangential components of force, respectfully. The torque τ on each particle is the sum of the moment of the tangential forces (Ft) arising from inter-particle contacts:

$$\sum \tau_i = r_i x \times F_i \ldots\ldots\ldots\ldots\ldots\ldots\ldots (2)$$

Table 1: Properties of monodisperse particles of diameter 2mm.

Density of beads (Kg/m^3)	2460, 2860	Total number of beads 87000 to 243000	
Young's Modulus (Pa)	5.0 ×10^6	Diameter of beads 2mm	
Poisson Ratio	0.45	Diameter of intruder 0.30mm	
Coefficient of Restitution	0.3	Height of Cylinder 250mm	
Time-step (sec)	0.00001	Diameter of Cylinder 150mm, 200mm & 250mm	

The normal force (Fn) is given by:

$$Fn = \frac{4}{3} E * \sqrt{R *}\, \delta_n^{3/2} \text{.....3}$$

Where δn is a function of normal overlap, E∗ is the equivalent Young's Modulus, and R* the equivalent radius, which are defined by:

$$\frac{1}{E^*} = \frac{1-v_i^2}{E_i} + \frac{1-vj2}{Ej} \text{.....4}$$

$$\frac{1}{R^*} = \frac{1}{R_i} + \frac{1}{Rj} \text{.....5}$$

with Ei, νi, Ri and Ej, νj, Rj are the Young's Modulus, Poisson ratio and radius of particle i and j in contact. Here, we use the open-source code LIGGGHTS [13], which is an improved version of LAMMPS [14] for general granular and granular heat transfer simulations.

1.2. Simulation Parameters

The simulations parameters set measured in SI units as shown in **Table 1** and **Table 2**. The packing is generated by pouring N mono-dispersed particles in from a fixed height and allowing them to rest under gravity. The interactions among the spheres and sphere-intruder are according to Hertzian history-dependent contact forces. In the first case, the testing system comprises 150000 mono-dispersed beads of diameter 2 mm and more details of the bead is shown in **Table 1**. The height of the cylinder is 25cm (125 Particle-Diameter) while its diameter is 20cm (100PD). The intruder velocity is fix at (10cm/sec). We found that the change in velocity has no effect on the trend of the force profile curve, in accordance with the previous force profile studies. In the second case, the testing carried out using rectangular box consists of 411500 mono-disperse particles of diameter 3mm. The detail of the particles is given in **Table 2**. The height of the box is 17.2cm (57.33PD) with width and length of 22.5cm (75PD). We used the same spherical intruder of wall type with diameter 30mm (10PD) is used and the velocity of intruder is 100mm/sec (33.33PD/sec).

2. Results and Discussion

In the first case the drag force experienced by spherical intruder moves vertically down in silo geometry. The drag force on intruder is due to the net force of granular particles. The direction of the force is opposite to the motion of an intruder. In the first case, the spherical intruder was allowed to move down in a granular column. Fig. 2 (a) shows the force profile on spherical intruder moving vertically down in granular packing in a silo of diameter 20cm.

Table 2: Properties of mono-disperse particles of diameter 3mm.

Density of beads (Kg/m3)	2860	Total number of beads	≈400000
Young's Modulus (Pa) $\times 10^6$	2.0	Diameter of beads	3 mm
		Diameter of intruder	30mm
Poisson Ratio	0.45	Height of Box	165mm
Coefficient of Restitution	0.3	Width & length of Box (mm)	255×225
Time-step (sec)	0.00001		

Frictions between wall-particles are 0.0, 0.2 and 0.5 while the density of the particles is 2460Kg/m^3. It is evident from **Fig 3** that drag force augment with the increase in friction values. It is also revealed from this figure that drag force suddenly increases when the intruder reaches near the base of the silo. The reason for this may be that particles in the path cannot move further when an intruder approaches near to the base so they apply larger force on both the wall and the intruder. In another words, force network of granular particles seems to strongly depend on friction values. Hence, most of the stresses are carried out due to the friction this is in accordance with the prediction of Janssen model [24]. The model predicts that in a silo most of the weight is screened by sidewalls and hence a little weight is transferred to the base of the container.

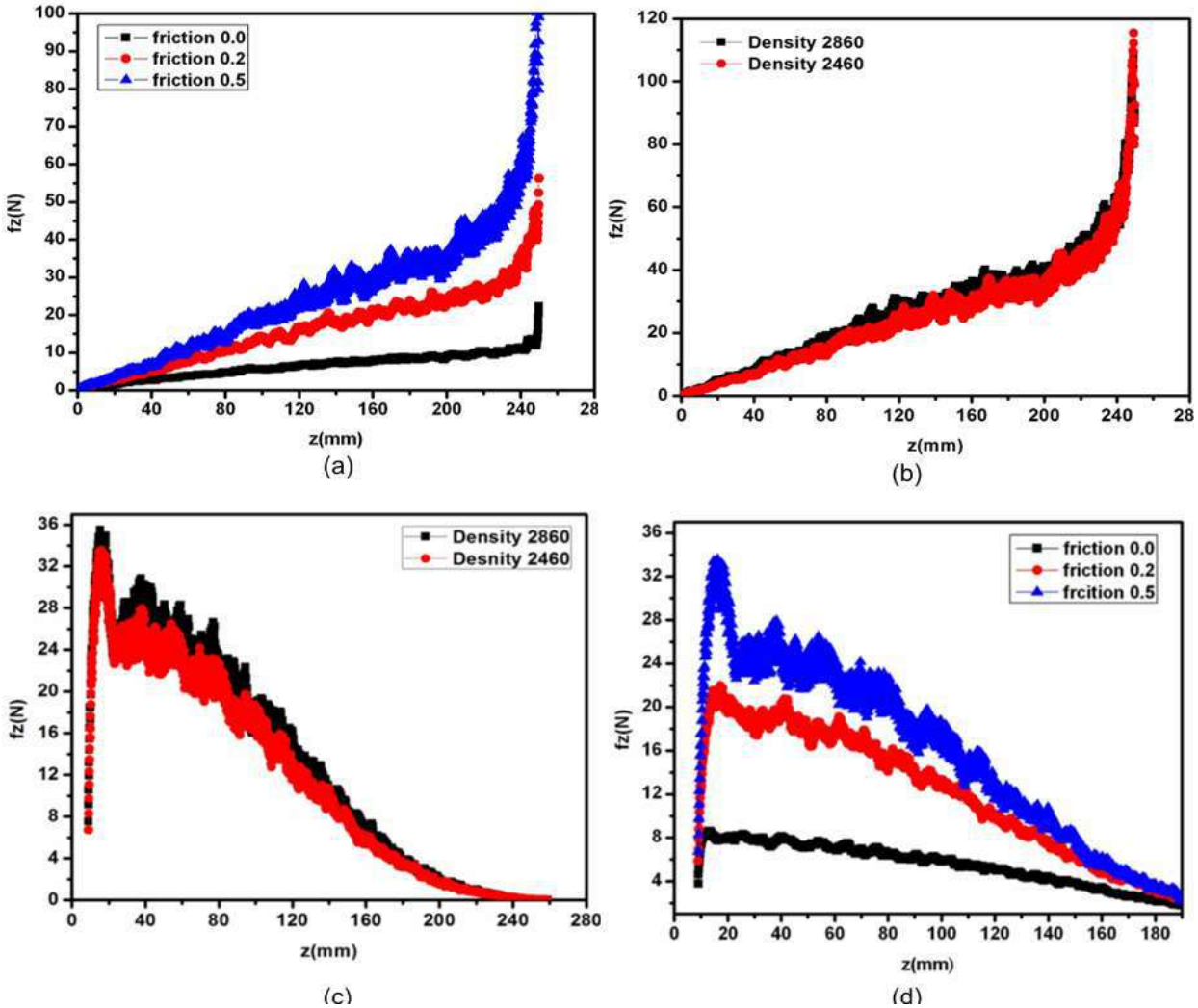

Fig. 2 (a) The variation of drag force as a function of different values of friction between the beads and silo. (b) Force profile on spherical intruder motion vertically down in granular packing in silo of diameter 20cm. (c) Force profile on spherical intruder motion up in granular packing in silo of diameter 20cm. in this case friction is kept constant and we used two types of particles of different densities. (d) Force profile on spherical intruder moving up in granular packing in a silo of diameter 20cm.

In the second case the simulation of the intruder was made to move vertically in a cylindrical granular column of diameter 20cm. In this case, friction between particles is constant while we use two types of particles of densities 2460Kg/m^3 and 2860Kg/m^3. The effect of drag force on the intruder is investigated in such a case. It is evident from **Fig. 2 (b)**

that the drag force is independent of the density of the material. However, the trend shows a similar behavior as depicted Fig. **2 (a).**

In the next simulation run, examined the effect of drag force on the intruder in the case where the intruder is moving vertically up in a silo of diameter 20 cm. **Fig 2 (c)** shows the results of drag force versus insertion depth in the case of varying density of grain material. Here the friction between the grains is kept constant and the density of the medium is changed. It is clear from this **Fig. 2 (d)** that on the inset of motion large drag force is experienced by the inserted object as it emerges out and reaches near the free surface the force decreases nonlinearly. It may be due to the reason that in the silo top weight is screed by the sidewall and hence the drag force decreases as the intruder goes up. Moreover, the contacts are enduring, therefore the particle inertial effects are negligible it is in accordance with the Janssen model this model is still used in designing of silos.

Hence it is revealed that the density of granular media does not significantly influence the drag force on penetrating objects in both the case, i.e when the intruder moves up or down in the vertical cylinder. Therefore, to explore the influence of friction on drag force we have carried out simulation where the friction parameter is varied. **Fig. 2 (d)** shows the dependence of drag force on friction between the beads and silo wall. In this case, the spherical intruder was moved up in a silo where the friction between wall-particles is 0.0, 0.2 and 0.5 while the density of the particles is uniform that the 2460Kg/m^3. We observed that force profile exhibits nonlinear decay, at the onset of motion larger drag is experienced as the intruder travels some distance upward the drag force reduces rapidly in all three situations.

It appears that near the bottom of silo weight of grain is transferred to the bottom, in other words, there is a negligible conversion of vertical stresses to the horizontal ones. Whereas on, the top conversion of vertical stresses to the horizontal ones is more pronounced. These conversions are due to the arch formation in silos [16]. Hence, it shows that larger the values of coefficient of friction lead to more stress conversion. In this way when the spherical intruder moves upward in a granular column with $\mu = 0.0$ there is an absence of stress conversion and hence it experiences the drag due to the top lying grains. Whereas when $\mu = 0.5$ the intruder has to break the horizontal arches as well, so the drag exhibits larger values as shown in **Fig. 2 (d).**

To further elaborate the influence of arches in cylindrical geometry, in the next simulation run the intruder is allowed to move vertically up in a granular column of diameters 15, 20 and 25cm. The force profile in such cases is shown in **Fig. 3 (a),** while the density of material and friction between particles have been kept constant. The force profile curves in such cases are identical and decay nonlinearly. The reason for this may be that the value of $\mu = 0.5$ has produced similar arches in each case and the intruder experience similar drag force as it moves up in silo. From the above discussion, it appears that in a granular column the arches are produced which becomes stronger as one goes up from the base of granular column [26].

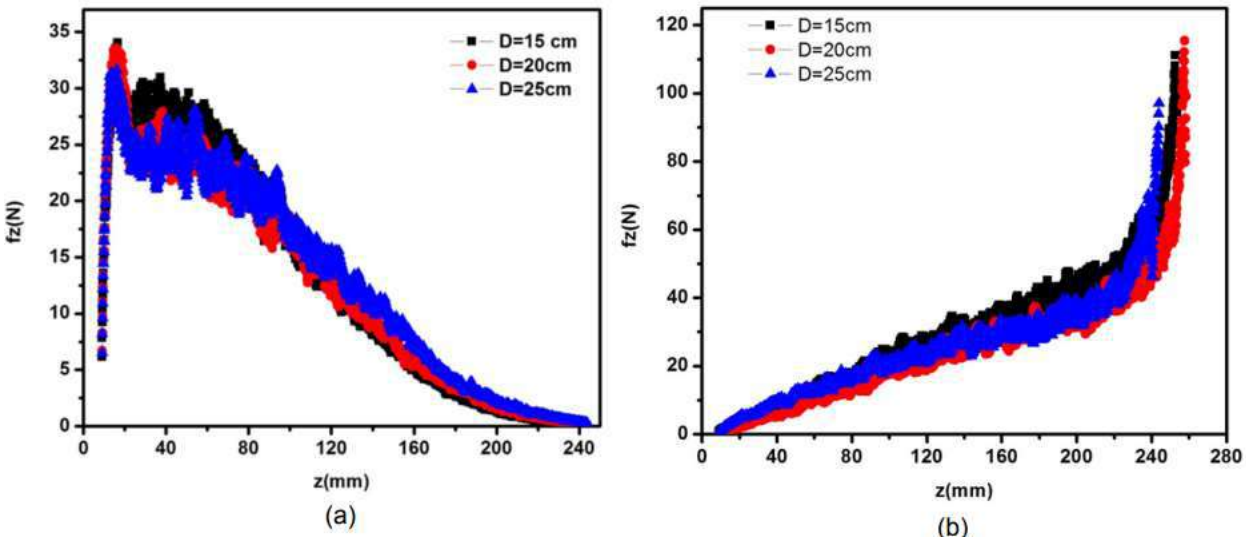

Fig. 3 (color online) (a) Force profile on spherical intruder moving up in granular packing. In this case, friction and density of the particles are constant while the diameter of silo is varied. (b) Force profile on spherical intruder motion down in granular packing. In this case, friction and density of the particles are constant while the diameter of silo is changed.

In order to further investigate the role of arch formation in a granular column we have varied the silo size while keeping the coefficient of friction and density of materials as constant. **Fig. 3 (b)** depicts the force profile of intruder moving down in silo having diameters 15cm, 20cm and 25cm, respectively. In all three cases, the friction between particles and density has been kept constant. It is evident from **Fig. 3 (a)** that curves are identical in each case. The nonlinear increase of force with the depth is interpreted as the intruder moves down to the base the particles in the path cannot move further so they

exert force on the base of the silo as well as on intruder and hence the force grows rapidly. It is also clear from this figure that curves are almost identical even the silo size has been changed. It may be due to the reason that the constant coefficient of friction resulted in the identical arch formation in each case and hence we get the same variation in force profile of the intruder.

In order to confirm and investigate the role of arches with the height, the intruder is moved from one side to the other side box at the bottom and in the middle of the rectangular box along the x-axis. The variation of force profile with the distance is shown in **Fig. 3 (a)**, also all the parameter are constant in both cases. From **Fig. 4**, it is evident that intruder experience a larger force when moving through the middle of the container than at the bottom. At the middle of the box, the intruder encounters strong arches and hence drag force is increased. Whereas near the bottom of the container the arches are not fully developed which is possibly the reason less drag force is experienced by the intruder. It appears that it is the presence of strong arches at the middle section of the box which leads to larger drag force to the intruder at the middle of the box than at the bottom of rectangular box.

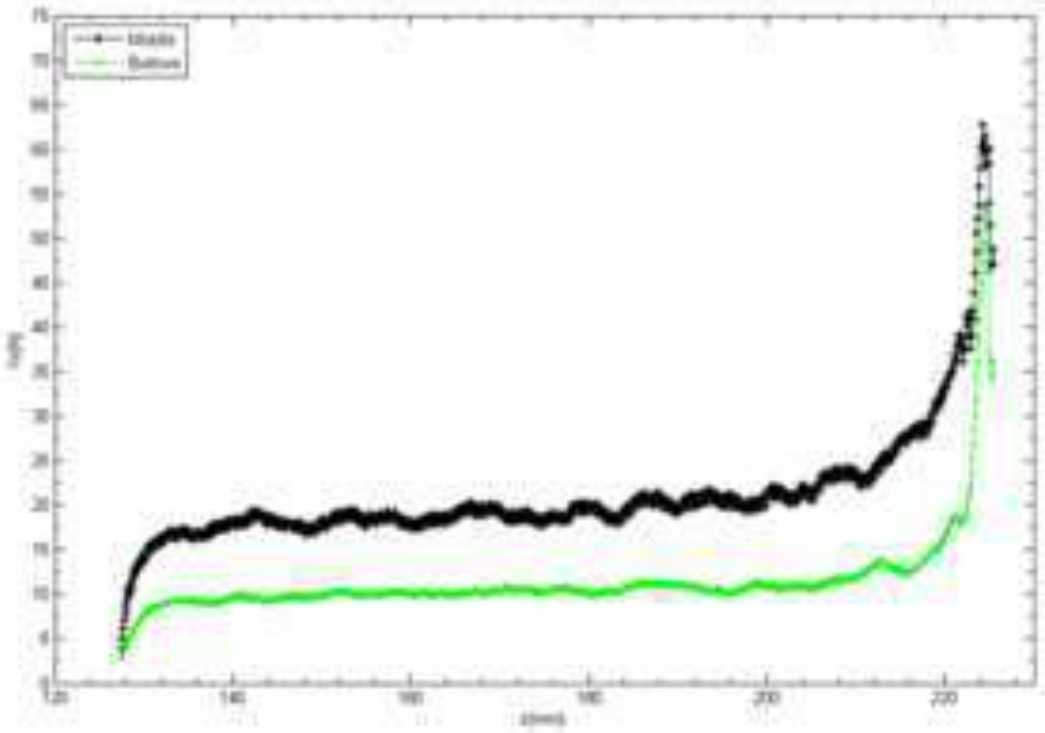

Fig. 4: Force profile on intruder motion along x-axis in granular packing of rectangular box.

3. Conclusion

In this paper, we numerically investigated the drag force, acting a spherical-shaped intruder moving in silo and rectangular geometry of granular column, by 3D DEM simulations.

It is revealed that drag force experienced by the horizontally and vertically motion of the intruder depends on the friction between the particle and container wall and is independent of the density of material and silo size. The dependency of drag force on friction is attributed to the arch formation in a silo. In future studies, this work will be

corroborated with the investigation of the influence of a number of contact points on drag and lift forces. It is expected that these results will be helpful to better understand the rheology of particulate media.

References

[1] Akinola M. Adesola. et al. 2017 Kuwait journal of science 44.

[2] Faten mustafa slaty. et al. 2019 Kuwait journal of science 46.

[3] Albert, I. et al. 2001 Physical Review E 64 4

[4] Ding, Y., Gravish, N. and Goldman, D. I. 2011 Physical Review Letters 106 1-4

[5] Soller, R. and Koehler, S. A. 2006 Physical Review E 74

[6] Albert, R. et al. 1999 Physical Review Letter 82 205?208

[7] Matthew B. Stone, David P. Bernstein, Rachel Barry, Matthew D. Pelc, Yee-Kin Tsui and Peter Schiffer 2004 Nature 427 503?504

[8] Stone, M. B, Barry, R., Bernstien, D. P., Pelc, M. D., Tsui, Y. K., and Schiffer, P. 2004 Physical Review E 70 10

[9] Janssen, H. A. 1895 Zeitschrift des Vereins Deutscher Ingenieure 39 1045-1049

[10] Chand, R., Khaskheli, M. A., Qadir, A., Ge, B. & Shi, Q. (2012) Physica A 391, 4590–4596.

[11] Chand, R., Muniandy, S. V., Wong, C. S. & Singh, J. (2017) Particuology 32, 890–894. [12] Cundall PA, Strack ODL 1979 Geotechnique 29 47-65

[13] Open source code LIGGGHTS : https://www.cfdem.com [14] Open source code LAMMPS : https://lammps.sandia.gov

[15] Peng, Z., Xu, X., Lu, K., and Hou, M. 2009 Physical Review E 80 1-5 8

[16] Amarouchene, Y., Boudet, J. F. and Kellay, H. 2001 Physical Review Letters 86 4286-4289

[17] Anamalamudi, S. et al. 2018 Elsevier B. V 83 228?238

[18] Boudet, J. F., Amarouchene, Y. and Kellay, H. 2008 Physical Review Letters 101

[19] Umbanhowar, P. and Goldman, D. I. 2010 Physical Review E 82 0?3

[20] de Bruyn, J. R. and Walsh, A. M. 2004 Canadian Journal of Physics 82 439-446

[21] Buchholtz, V. and Poschel, T. 1998 Granular Matter 1 33-41

[22] Cavarretta, I., Coop, M. and O?Sullivan, C. 2010 Geotechnique 60 413-423

[23] Goldman, D. I. and Umbanhowar, P. 2008 Physical Review E 77

[24] Lohse, D. et al. 2004 Nature 432 689?690

[25] Pipatpongsa, T. and Heng, S. 2010 Journal of Solid Mechanics and Materials Engineering 4 1237-1248

[26] Widisinghe, S. and Sivakugan, N. 2014 International Journal of Geotechnical Engineering 8 431?435

[27] Zhou, Y. et al. 2018 Kuwait Journal of Science 45 94?103

[28] Zhu, H. P. et al. 2004 Granular Matter 5 193?199